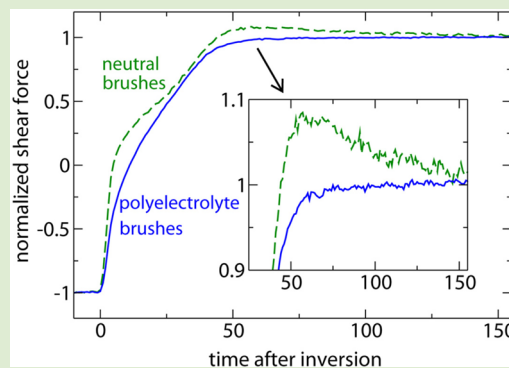


Strongly Compressed Polyelectrolyte Brushes under Shear

L. Spirin^{†,‡} and T. Kreer^{*,‡}[†]Graduate School Materials Science in Mainz, Staudingerweg 9, 55128 Mainz, Germany[‡]Leibniz Institut für Polymerforschung Dresden, Hohe Straße 6, 01069 Dresden, Germany

ABSTRACT: By means of molecular dynamics simulations we provide evidence for pronounced counterion immobilization in strongly compressed polyelectrolyte-brush bilayers, where the counterions represent the vast majority of mobile solvent particles. As a consequence, hydrodynamic effects are strongly suppressed and semidilute bilayers can respond to shear motion like electrically neutral bilayers at melt density. For large, time-independent shear rates, $\dot{\gamma}$, the shear force scales as $f(\dot{\gamma}) \sim \dot{\gamma}^{0.69}$, in agreement with scaling theory. In this regime, polyelectrolyte-brush bilayers can stabilize highly nonstationary processes, such as the instantaneous inversion of the shear direction. The absence of hydrodynamic flow leads to a suppression of the overshoot for the shear force, which is found for electrically neutral bilayers with the same molecular parameters. We suggest that nature uses this mechanism to optimize biolubrication, for instance in synovial joints.



The upcoming desire to control fluid flows on extremely small scales, as for instance in biomimetic nanotechnology, demands a deep understanding of hydrodynamic effects on the micro- and nanoscale. An important example are microchannels covered with polyelectrolyte brushes (PEBs), which are of great relevance in biomechanical transport processes, such as synovial joint lubrication or flows through capillaries of plants or blood vessels. Therefore, PEBs currently are in the focus of many experimental,^{1,2} theoretical,³ and numerical^{4–6} studies.

PEB bilayers, which consist of two PEBs facing each other, display extremely small kinetic friction in relative sliding motion.^{1,2} To a large extent, the nonlinear response of strongly compressed, electrically neutral polymer-brush bilayers to shear recently has been explained via scaling theory,^{7,8} while a clear picture of PEB bilayers under shear has not emerged to date. Certain progress has been made for weakly compressed bilayers, where the electrostatic interactions are known to hamper the mutual brush interpenetration,³ leading to small friction forces. Simultaneously, the osmotic pressure of the counterion cloud between the two brushes may carry relatively large normal loads.⁵

In this Letter, we focus on the regime of strongly compressed PEB bilayers, which is of particular importance, for example, for human knee joints, where pressures up to 50 atm have to be sustained by the synovial fluid. The bilayers are compressed such that the total monomer density of the brushes is homogeneous, while the system is still semidilute. In this regime, the opposing brushes and their counterion clouds interact strongly. Using molecular dynamics (MD) simulations of a classical numerical model, we demonstrate a pronounced counterion immobilization (CI) for surprisingly small values of the Bjerrum length, λ_B .⁹ The response to both steady and

nonstationary shear then is comparable to electrically neutral bilayers at melt density, where hydrodynamic effects are absent. When the direction of shear is quasi-instantaneously inverted, CI results in the suppression of an overshoot for the shear force, which occurs for neutral, semidilute bilayers.^{10,11}

Figure 1 shows the steady-state shear force, $f(\dot{\gamma})$, as a function of shear rate, $\dot{\gamma}$, for different values of λ_B . As described below, the latter is varied by modification of the dielectric constant of the medium. We divided $f(\dot{\gamma})$ by the power-law expected for

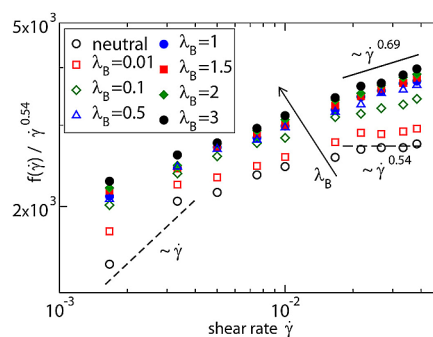


Figure 1. Shear force, divided by the expected power-law behavior of electrically neutral, semidilute bilayers at large constant shear. Our data are shown on a double-logarithmic plot for different values of the Bjerrum length (increasing in the direction indicated by the arrow). The solid line results from a fit through the last four points of all data sets with $\lambda_B \geq 0.1$. The error bars are smaller or equal to the symbol size.

Received: September 27, 2012

Accepted: December 14, 2012

Published: December 28, 2012

neutral, semidilute bilayers in the nonlinear regime,^{7,8} $f(\dot{\gamma}) \sim \dot{\gamma}^{0.54}$, such that we obtain an (almost) horizontal line for large shear rates. For small values of $\dot{\gamma}$, bilayers with $\lambda_B \leq 0.01$ reveal a regime of linear response, where $f(\dot{\gamma}) \sim \dot{\gamma}$. This regime is absent for $\lambda_B \geq 0.1$, where the electrostatic interactions lead to a nonlinear response of the bilayer even for our smallest shear rates. For large shear rates, a new power-law, $f(\dot{\gamma}) \sim \dot{\gamma}^{0.69}$, is established, which corresponds to our recent prediction^{7,8} for neutral bilayers at melt density, indicating that hydrodynamic effects must be strongly suppressed. Moreover, the shear force increases with λ_B , revealing that PEB bilayers under strong compression dissipate more kinetic energy than their neutral counterparts with the same molecular parameters. However, we demonstrate below the advantage of PEBs to stabilize the response during nonstationary shear motion. We provide evidence that this phenomenon and the new power-law are a consequence of pronounced CI and the concomitant suppression of hydrodynamic effects in strongly compressed PEB bilayers.

Our numerical data stem from MD simulations of a classical bead–spring polymer model,¹² where the excluded volume interaction is mimicked with a Lennard-Jones potential and the connectivity along the backbone of a polymer chain is assured via the FENE potential. We use the same approach as for previous studies of electrically neutral bilayers.^{7,8,10,11} Linear polymer chains, each of length $N = 30$, are grafted with one end onto flat surfaces. Our grafting density, $\sigma_g \approx 0.17$ (Lennard-Jones units), is slightly larger than twice the overlap grafting density, at which electrically neutral polymers start to form brushes. The grafting surfaces are placed parallel to each other at a distance $D = 14.24\sigma$ (σ the monomer diameter). After filling the system with dimers (polymer chains of length $N = 2$) up to a total monomer (brush and solvent) number density of $\rho = 0.9$, we obtain a bilayer well in the semidilute regime.^{7,8} To introduce electrostatic interactions, we assign a charge of $-e$ to a fraction $q = 1$ of the brush monomers and add counterions (monomers of charge $+e$) to neutralize the system.¹³ Still, the number of neutral solvent dimers is chosen such that $\rho = 0.9$. All particles interact with the same excluded volume interaction. We integrate Newton's equations of motion with the Velocity-Verlet algorithm¹⁴ and standard Ewald summation¹⁵ to account for the long-range character of the electrostatic interaction. The latter incorporates electrostatic interactions via an unscreened Coulomb potential. Using a Dissipative Particle Dynamics thermostat,¹⁶ temperature is kept at a value of $T \approx 1.7k_B$, where k_B denotes the Boltzmann constant.

Different strategies can be chosen to vary the strength of electrostatic interactions. Let us consider a screened Coulomb potential as the effective pair potential between charged point particles at distance r , $V(r) \sim k_B T \lambda_B \exp(-r/\lambda_D)/r$. With c_i the concentration of ions with valency z_i , the screening (Debye) length can be expressed in terms of λ_B via $\lambda_D = 1/4\pi\lambda_B \sum_i c_i z_i^2$, where the Bjerrum length is given as $\lambda_B = e^2/4\pi\epsilon_0\epsilon_r k_B T$.¹⁷ Here, ϵ_0 and ϵ_r , respectively, denote the vacuum permittivity and the dielectric constant of the medium.

To study the influence of the Coulomb interaction, one may vary the salt concentration, which modifies the screening length, leaving the prefactor in $V(r)$ constant. However, the salt concentration cannot be varied to a large extent for a strongly compressed bilayer. Alternatively, one may change the temperature, which also yields a constant prefactor in $V(r)$, but then one studies systems at different thermodynamic

conditions. Here, we apply a third method, namely the variation of the dielectric constant.

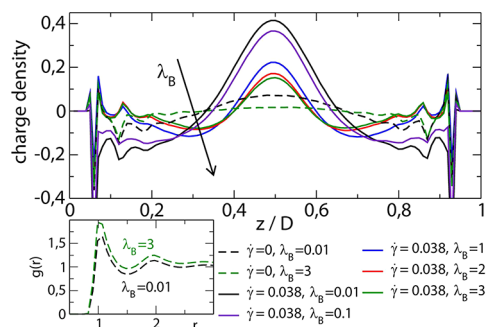


Figure 2. Charge density distribution, defined as the difference between the number densities of unlikely charged particles (z the direction orthogonal to the grafting surfaces). Lower part: Monomer-counterion pair correlation function for $\lambda_B = 0.01$ and 3.

Starting out from a neutral bilayer ($\lambda_B = 0$), increasing the Bjerrum length leads to an increase of the prefactor in $V(r)$ and to a decrease of λ_D . Finally, this results in a strong CI (see Figure 2). We show the difference between the number density distributions of unlikely charged ions throughout the bilayer. Upon increasing values of λ_B , we observe smaller oscillations of the charge distribution. This applies both for steady-state shear and for static equilibrium ($\dot{\gamma} = 0$), where a pronounced CI is found at $\lambda_B = 3$. At large shear, the grafted chains incline and stretch along the shear direction to reduce their mutual overlap.^{7,8} Due to the concomitant densification of the brushes, more counterions accumulate in the interpenetration zone of the brushes than at zero shear. This behavior is well documented for solvent molecules in neutral bilayers.⁷

The effect of CI modifies the response of PEB bilayers to shear dramatically. The counterions resist strongly against being pushed out of deeper brush layers into the interpenetration zone. Upon increasing values of λ_B , they lose their identity as mobile, solvent-like particles and become part of monomers with a somewhat larger effective size. This effect is reflected by the monomer-counterion pair correlation function, as can be seen in the lower part of Figure 2. For strongly compressed bilayers, where the counterions represent the majority of mobile particles, this leads to a suppression of hydrodynamic effects and to a crossover from a semidilute system to a bilayer at melt density.

Former studies^{7,8,10,11} indicated that both conformational and collective responses to shear are determined by the amount of mutual brush interpenetration. The latter can be characterized via the width, L , of the Gaussian distribution, which is obtained when the monomer density profiles of the two brushes are multiplied (see Figure 3a and ref 18). For strongly compressed bilayers at melt density, the interpenetration width reads^{7,19,20}

$$L_m \approx \left(\frac{N^2 b^4}{D} \right)^{1/3} \quad (1)$$

where b denotes an effective monomer size. Scaling arguments⁷ suggest that this yields a friction force that scales as $f(\dot{\gamma}) \sim \dot{\gamma}^{0.69}$ in the nonlinear regime, which is in agreement with our data for $\lambda_B \geq 0.1$ (Figure 1). On the other hand, one obtains⁷

$$L_s \approx a \left[N^{2\nu} (\sigma_g a^2)^{2(1-2\nu)} \left(\frac{a}{D} \right)^{1-\nu} \right]^{1/3(3\nu-1)} \quad (2)$$

for the interpenetration width of semidilute bilayers, where a denotes the effective monomer size in the semidilute regime and $\nu \approx 0.588$, the Flory exponent.²¹ For large shear, this leads to $f(\dot{\gamma}) \sim \dot{\gamma}^{0.54}$,⁷ corresponding to the horizontal line in Figure 1. We conclude that, upon increasing the Bjerrum length, our semidilute bilayers undergo a transition to effectively neutral bilayers at melt density due to CI.

Surprisingly, the crossover between the two regimes is rather sharp, that is, the exponent in Figure 1 changes rather abruptly. For intermediate values of λ_B , one should expect that electrostatic interactions are relevant, while the Debye length still exceeds the screening length, ξ , of the excluded volume interaction.²¹ Once the Bjerrum length is above a critical value, λ_B^c , the Debye length is smaller than ξ , and the excluded volume interaction dominates.

With the parameters corresponding to the data shown in Figure 1, we find that electrostatic interactions should be relevant for $\lambda_B \leq \lambda_B^c \approx 0.02a$.²² This value is within the regime, where we observe the crossover from semidilute to melt behavior (see Figure 1). Thus, only weakly charged, semidilute PEB bilayers at strong compression can display a broad intermediate regime. In fact, if only one monomer per chain is charged, that is, $q = 1/30$, we obtain a value for λ_B^c close to the Bjerrum length of (bulk) water, which is $\lambda_B \approx 0.7\sigma$, for our numerical model.²³

While the above considerations explain the sharp crossover of the response for neutral, semidilute bilayers to effectively neutral bilayers at melt density and the corresponding power-laws of the shear force at large shear rates, we still have to clarify why we observe larger friction forces upon increasing values of λ_B . Keeping in mind that $f(\dot{\gamma})$ is closely related to the mutual brush interpenetration, one may compare the expressions given in eqs 1 and 2, that is,

$$\frac{L_m}{L_s} \approx (ca^3)^{2(2\nu-1)/3(3\nu-1)} \left(\frac{b}{a} \right)^{4/3} \quad (3)$$

Demanding $L_m/L_s > 1$ yields, with $\nu \approx 3/5$, the condition $ca^3 > (a/b)^8$. The effective monomer size for bilayers with CI should be (at least) twice the monomer size for neutral bilayers, thus, we obtain $ca^3 > 1/256$. This condition is always fulfilled for a semidilute bilayer. Because we anticipated already that the crossover regime is rather narrow and not resolved for the values of λ_B considered here, we expect a monotonic increase of L upon increasing Bjerrum length.

In fact, this behavior can be observed in Figure 3b, both at static equilibrium and at our largest shear rate. It is rather inconvenient to measure L explicitly in the simulation. Instead, we monitor the binary interbrush monomer contacts, N_{int} , by counting the number of excluded volume interactions taking place between monomers of different brushes. This method has been applied successfully in several previous studies, for instance, in refs 7, 10, 11, and 18.

Figure 3c reveals a slower decrease of $N_{\text{int}}(\dot{\gamma})$ for larger Bjerrum lengths. This finding is consistent with the increase in the shear force and the exponent observed in Figure 1. However, it seems surprising that electrostatic interactions lead to larger friction forces, while many biological systems contain polyelectrolytes. We have made a similar observation for neutral bilayers with macromolecular inclusions.^{10,11} Also, here,

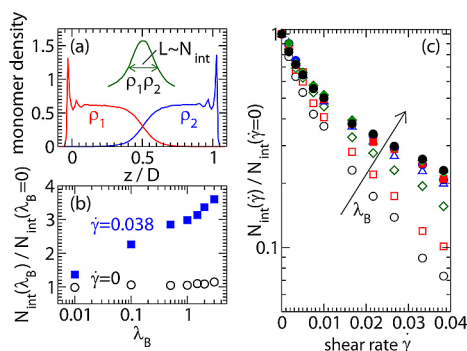


Figure 3. (a) When the monomer number densities of both brushes are multiplied, we obtain a Gaussian distribution, which is used to define the interpenetration width. The latter is (roughly) proportional to the number of binary interbrush monomer contacts. (b): N_{int} rescaled by its value for a neutral bilayer, as a function of the Bjerrum length. (c) N_{int} rescaled by its value at static equilibrium as a function of shear rate for different Bjerrum lengths. Same legend as Figure 1.

the resistance to shear is larger for systems with inclusions than for pure bilayers, despite biological systems often contain such inclusions.

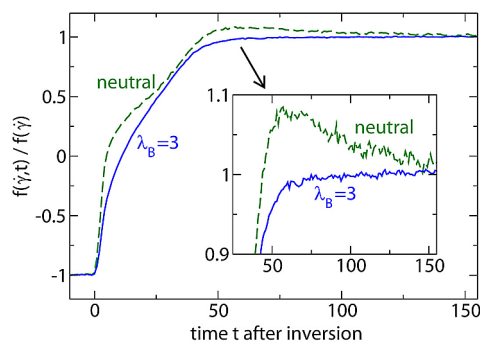


Figure 4. Time development of the shear force divided by its steady-state value during shear inversion at time $t = 0$.

Nature provides fascinating solutions to optimize lubrication processes. A typical shear motion, for instance occurring in a mammalian knee joint during walking, rarely invokes shear rates that are constant in time. Instead, the motion is often rather abrupt and invokes highly nonstationary shear fields. Experiments²⁴ and simulations^{10,11} indicate that pure, electrically neutral bilayers exhibit mechanical instabilities, for instance an overshoot of the shear force, during nonstationary shear motion. Recently,^{10,11} we could demonstrate that macromolecular inclusions stabilize the response of neutral bilayers when the direction of shear is quasi-instantaneously inverted. It is tempting to conclude that nature uses this mechanism in synovial joint lubrication.

As can be seen from Figure 4, a similar conclusion may be drawn for the influence of electrostatic interactions on polymer-brush lubrication. Starting out from a steady-state configuration at our largest shear rate, we invert the shear direction on a time scale that is small compared to the relevant relaxation time of the bilayer.^{10,11} In this way, we simulate half a cycle of large amplitude oscillatory shear (LAOS), as it is typically performed in experiments. For neutral bilayers, the shear force changes rather abruptly and exhibits an overshoot before the inverted steady state establishes. On the other hand, our PEB bilayer

with $\lambda_B = 3$ reveals a much smoother transition without the occurrence of an overshoot.

The explanation for this finding should be related to the pronounced CI and the suppression of hydrodynamic effects in strongly compressed bilayers. Let us recall the picture developed for neutral bilayers.^{10,11,18} At large constant shear, the grafted chains are stretched and inclined along the shear direction, while solvent molecules are pushed out of deeper brush layers into the interpenetration zone. In this way, mutual brush interpenetration and friction are reduced. When the shear direction is inverted, the chains have to undergo a transition, in which they change their inclination toward the new shear direction. During this process, solvent molecules flow back into deeper brush layers and the width of the interpenetration zone increases, resulting in the overshoot of the shear force.¹¹ However, our previous studies also revealed the absence of the overshoot when solvent molecules are not explicitly taken into account. This indicates that hydrodynamic effects are essential for the occurrence of mechanical instabilities. Thus, the smooth crossover we observe for the PEB bilayer in Figure 4 is in perfect accordance with the response of a neutral bilayer at melt density. Compared to the neutral solvent, immobilized counterions are far less accumulated in the overlap region, such that the effect of backflow and the overshoot during shear inversion are strongly reduced.

It may be concluded that this mechanism, together with the advantages provided by macromolecular inclusions, is an important strategy of nature to optimize biolubrication and may be of use for technical applications. Thus, aiming at the minimization of friction between surfaces in relative shear motion, future investigations should address the interplay between electrostatic interactions and macromolecular inclusions. The more complex geometry of biological polyelectrolytes can produce a wider variety of behavior with more than one mechanism as a source.

AUTHOR INFORMATION

Corresponding Author

*E-mail: kreer@ipfdd.de.

Notes

The authors declare no competing financial interest.

ACKNOWLEDGMENTS

We are grateful to the “Exzellenzinitiative des Bundes und der Länder” and the German Science Foundation (DFG-Kr 2854/3-1) for financial support. Furthermore, we appreciated discussions with C. Pastorino, A. Johner, and J.-U. Sommer. In addition, we thank D. Adam for her help during preparation of the manuscript.

REFERENCES

- (1) Raviv, U.; Giasson, S.; Kampf, N.; Gohy, J. F.; Jerome, R.; Klein, J. *Nature* **2003**, *425*, 163; *Langmuir* **2008**, *24*, 8678.
- (2) Dunlop, I. E.; et al. *J. Phys. Chem. B* **2009**, *113*, 3947.
- (3) Matsen, M. W. *Eur. Phys. J. E* **2011**, *34*, 45; **2012**, *35*, 13.
- (4) Carrillo, J.-M. Y.; Russano, D.; Dobrynin, A. V. *Langmuir* **2011**, *27*, 14599.
- (5) Ou, Y.; Sokoloff, J. B.; Stevens, M. J. *Phys. Rev. E* **2012**, *85*, 011801.
- (6) Goujon, F.; Ghoufi, A.; Malfreyt, P.; Tildesley, D. J. *Soft Matter* **2012**, *8*, 4635.
- (7) Galuschko, A.; et al. *Langmuir* **2010**, *26*, 6418.

(8) Spirin, L.; Galuschko, A.; Kreer, T.; Johner, A.; Baschnagel, J.; Binder, K. *Eur. Phys. J. E* **2010**, *33*, 307.

(9) λ_B defines the distance over which the electrostatic potential decays to the typical strength of thermal fluctuations.

(10) Spirin, L.; Galuschko, A.; Kreer, T.; Binder, K.; Baschnagel, J. *Phys. Rev. Lett.* **2011**, *106*, 168301.

(11) Spirin, L.; Galuschko, A.; Kreer, T. *Macromolecules* **2011**, *44*.

(12) Kremer, K.; Grest, G. S.; Carmesin, I. *Phys. Rev. Lett.* **1988**, *61*, 566.

(13) We perform our simulations at zero salt concentration.

(14) Swope, W. C.; Andersen, H. C.; Berens, P. H.; Wilson, K. R. *J. Chem. Phys.* **1982**, *76*, 648.

(15) Darden, T.; York, D.; Pedersen, L. *J. Chem. Phys.* **1993**, *98*, 10089.

(16) Hoogerbrugge, P. J.; Koelman, J. M. V. A. *Europhys. Lett.* **1992**, *19*, 155.

(17) With our model parameters, we find $\lambda_D \approx 0.24\sigma^{3/2}\lambda_B^{-1/2}$.

(18) Kreer, T.; Binder, K.; Müser, M. H. *Langmuir* **2003**, *19*, 7551.

(19) Witten, T. A.; Leibler, L.; Pincus, P. A. *Macromolecules* **1990**, *23*, 824.

(20) Milner, S. T.; Witten, T. A. *Macromolecules* **1992**, *25*, 5495.

(21) de Gennes, P. G. *Scaling Concepts in Polymer Physics*; Cornell University Press: New York, 1979.

(22) We may calculate λ_B^c from $\lambda_D(\lambda_B^c) = \xi$, that is,

$$(4\pi\lambda_B^c \sum_i c_i z_i^2)^{-1/2} \approx a(ca^3)^{\nu/(1-3\nu)},$$

where we used the common expression $\xi \approx a(ca^3)^{\nu/(1-3\nu)}$.²¹ Assuming monovalent counterions balance the fraction q of charged brush monomers with total monomer concentration c , one can replace the sum via $\sum_i c_i z_i^2 = 2cq$, such that

$$\lambda_B^c \approx \frac{a}{8\pi q} (ca^3)^{(1-\nu)/(3\nu-1)}$$

(23) Csajka, F. S.; van der Linden, C. C.; Seidel, C. *Macromol. Symp.* **1999**, *146*, 243.

(24) Tadmor, R.; Janik, J.; Klein, J.; Fetters, L. J. *Phys. Rev. Lett.* **2003**, *91*, 115503.